JOURNAL OF SOLID STATE CHEMISTRY **135,** 132–139 (1998)
ARTICLE NO. SC977611

Oxygen Nonstoichiometry in Li–Mn–O Spinel Oxides: A Powder Neutron Diffraction Study

P. Strobel,* F. Le Cras,*,† L. Seguin,‡ M. Anne,* and J. M. Tarascon‡

* *Laboratoire de Cristallographie, CNRS, B.P. 166, 38042 Grenoble Cedex 9, France*; † *Commissariat à l'Energie Atomique, CEREM/DEM, 38054 Grenoble Cedex 9, France*; *and* ‡ *LRCS, Université de Picardie Jules Verne, 80039 Amiens Cedex, France*

Received April 23, 1997; in revised form September 2, 1997; accepted September 3, 1997

Neutron powder diffraction has been carried out on two series of Li–Mn–O samples with spinel structure, which have been shown to lose oxygen with respect to initial stoichiometric spinels: (i) $Li_{1.05}Mn_2O_4$ quenched from 800 or 925°C, (ii) "$Li_{1.33}Mn_{1.67}O_4$" (nominal) treated with ammonia gas at 200°C. The structural refinements unambiguously show that both 925°C quenching and low-temperature ammonia treatment induce oxygen vacancies in the spinel lattice. However, the mechanism of oxygen loss is markedly different between quenchings at 800 and 925°C. While the latter actually corresponds to the introduction of anionic vacancies at constant cation composition, the former is due to a rearrangement of the Li/Mn ratio in the spinel phase and the formation of an additional lithium-rich phase Li_2MnO_3. The presence of vacancies induce a significant increase in atomic displacement parameters of oxygen.

INTRODUCTION

The Li–Mn–O spinel system has been widely studied in the search for good cathode materials for rechargeable lithium batteries (1, 2). Cation-defective spinel phases have been known in this system for many years, following the discovery of λ-MnO_2 (3) and $Li_2Mn_4O_9$, the latter corresponding to $Li_{1-\delta}\square_\delta[Mn_{2-2\delta}\square_{2\delta}]O_4$ in spinel notation (4). The electrochemical capacity on lithium intercalation depends on the stoichiometry of the host spinel phase, which can be varied in several ways: (i) by varying α along the solid solution $Li_{1+\alpha}Mn_{2-\alpha}O_4$, within the limits $0 \leq \alpha \leq 1/3$ (corresponding to the manganese valence range $+3.5 \leq \nu(Mn) \leq +4$), (ii) by introducing cationic vacancies. Cation-vacant compositions are attractive for lithium intercalation on the so-called 3 V electrochemical reaction, which corresponds to the filling of octahedral sites in the spinel structure, with increased capacity in the case of a cation-deficient host material (1, 5).

Another kind of defect composition in this system has been suggested recently, following the observation of reversible oxygen loss in $Li_{1.05}Mn_2O_4$ by Tarascon *et al.* (6). This effect, which was confirmed and studied in more detail by Sugiyama (7) and Thackeray (8), is accompanied by a reversible phase transition between cubic and tetragonal forms and was ascribed to the occurence of oxygen atom vacancies in the structure. This hypothesis was further substantiated by Richard *et al.* (9), who reported a similar effect induced by low-temperature annealing of $Li_{1.33}Mn_{1.67}O_4$ in gaseous ammonia.

The only available structural investigations on the oxygen-vacant phases are powder X-ray diffraction studies. These do not allow accurate determination of the site occupancies of light atoms such as lithium (or even oxygen) in the presence of manganese. In addition, anion vacancies in the spinel structure, which is based on a cubic compact anionic network, have never been reported previously to our knowledge. For these reasons, powder neutron diffraction experiments were undertaken on several Li–Mn–O samples in which cationic or anionic vacancies are expected to occur. This paper presents the results of this neutron diffraction study on two such systems: $Li_{1.05}Mn_2O_{4-\delta}$ quenched from high temperature and $Li_{1+\alpha}Mn_{2-\alpha}O_{4-\delta}$ with α close to 0.33 treated by ammonia gas.

EXPERIMENTAL

The synthesis and annealing of $Li_{1.05}Mn_2O_{4-\delta}$ have been described previously (6). The starting materials γ-MnO_2 and Li_2CO_3 were initially reacted at 800°C. Quenching was achieved by quickly removing the powder from the hot furnace and pressing it between two cold stainless steel plates. These samples will be called thereafter by the letter 'T' followed by the annealing temperature and one or two letters (SC = slow-cooled, Q = quenched). Samples investigated here are T800SC, T800Q, and T925Q.

Another oxygen-deficient sample, $Li_{4/3}Mn_{5/3}O_{4-\delta}$, was prepared following the procedure of Richard *et al.* (10). An initial sample with overall stoichiometry $Li_{4/3}Mn_{5/3}O_4$ was prepared at 400°C from β-MnO_2 and $LiOH \cdot H_2O$: it will be named "C" throughout this paper. Its formula is given here

0022-4596/98 $25.00

TABLE 1
Characterization of Samples Used in This Study

Name	T800SC	T925Q	C	CN
Nominal Li/Mn ratio	0.525	0.525	0.75	0.75
Treatment	Slow-cooled	Quenched	—	200°C, NH_3(g)
Mn valence		($\Delta v = 0.32^a$)	3.92[b]	3.69[b]
X-ray cell parameters (Å)	8.226(6)	$a = 8.1155(9)$ $c = 8.649(2)^c$	8.1465(14)	8.154(9)

[a] From thermogravimetry.
[b] From chemical analysis.
[c] Tetragonal unit cell (data from Ref. (6) for quenching from 905°C).

in brackets, because the solid solution end member with $\alpha = 1/3$, corresponding to $v(\mathrm{Mn}) = +4.0$ was not obtained. As shown elsewhere (10, 11), this stoichiometry is not attainable as a pure phase. No sample with this nominal stoichiometry is single-phase: all samples reported contain Li_2MnO_3 as an impurity phase and have a lower α value than the 1/3 limit, with a maximum manganese oxidation state ≈ 3.9. Sample CN (for ammonia-treated) was obtained by heating sample C in flowing ammonia gas for 3 h at 200 ± 20°C, resulting in a mass loss of $\approx 3.0\%$.

Preliminary characterization was carried out by X-ray diffraction using a Siemens D-5000 powder diffractometer equipped with a diffracted-beam monochromator and operated with Cu$K\alpha$ radiation. Samples were analyzed both for total manganese and for manganese oxidation state by standard volumetric techniques. The X-ray characteristics and manganese valences are given in Table 1, for both parent compounds and nonstoichiometric spinel samples.

Neutron diffraction was carried out on the high-resolution two-axis D2B diffractometer of Institut Laue–Langevin, Grenoble, at wavelength 1.5945 Å. Samples were enclosed in vanadium containers with i.d. 9 or 16 mm, filled to a 70 mm height (corresponding to ≈ 6 and 15 g, respectively). Diffraction patterns were collected from 1° to 162° 2θ with 0.05° step and a total counting time of 6 h per sample. The structures were refined from neutron powder diffraction data using the whole-pattern-fitting Fullprof program (12) (Rietveld method).

RESULTS

1. Starting Model

The well-known spinel structure AB_2O_4 crystallizes in space group $Fd\bar{3}m$ (No. 227). Oxygen atoms occupy 32*e* sites with one variable position parameter $x(\mathrm{O}) = y(\mathrm{O}) = z(\mathrm{O})$. Cations *A* and *B* both occupy special positions with no variable position parameter. *A*, in position 8a, and *B*, in 16c, are tetragonally and octahedrally coordinated by oxygen, respectively. Mixed cation occupation, especially on *B*-sites, is common, as in $Li_{1+\alpha}Mn_{2-\alpha}O_4$, where a fraction α of the *B* (octahedral) sites is occupied by *A* atoms, such as lithium in this example. A change in cation distribution also changes the oxidation state of manganese, which is equal to $(7 - \alpha)/(2 - \alpha)$.

A spinel is stoichiometric if the cation/anion ratio M/O is 3/4. This criterion, which is independent of occupancy normalization, will be used to ascertain whether a given sample is stoichiometric, cation-deficient ($\mathrm{M/O} < 3/4$) or oxygen-deficient ($\mathrm{M/O} > 3/4$). For sufficiently high fractions of Mn^{3+}, manganese-containing spinel oxides are known to be distorted due to the Jahn–Teller effect associated with the d^4 electron configuration of trivalent manganese (1). This yields the hausmannite (Mn_3O_4) structure, with space group $I4_1/amd$ and volume halved with respect to the initial cubic structure.

2. Quenched $Li_{1.05}Mn_2O_{4-\delta}$ Samples

All samples studied gave powder patterns indexable in the cubic or tetragonal cells indicated above. The results of Rietveld refinements from neutron powder diffraction data on samples quenched from 800 and 925°C are given in Table 2, together with those for the parent (slow-cooled) compound. Observed and calculated neutron diffraction patterns are shown in Fig. 1.

Sample T800SC. This compound is a normal, cubic spinel. The refined lattice parameter is very close to the X-ray value (8.223 Å) and that corresponding to the nominal stoichiometry along the $Li_{1+\alpha}Mn_{2-\alpha}O_4$ solid solution (11, 13). The initial stoichiometry of this sample (Li/Mn slightly larger than 0.5) prompted us to introduce a mixed occupation of 16c octahedral sites by lithium and manganese, with the constraint of sites fully occupied. It converged to 0.06 Li + 0.94 Mn on this site ($\alpha = 0.12$), in fairly good agreement with the chemical composition. The oxygen occupancy on 32e site was also freed and did not shift significantly from full occupation. The isotropic displacement parameters are fairly large for tetrahedral lithium and oxygen atoms, which could be an effect of the mixed cationic occupation ($\alpha \neq 0$).

Sample T800Q. This sample is still cubic, but exhibits significant differences with respect to the slow-cooled one. The lattice parameter increased significantly to 8.250 Å (X-ray value: 8.245 Å), and an impurity phase, namely Li_2MnO_3, is weakly but significantly detected in the diffraction pattern (see Fig. 1b). A two-phase refinement showed that the lithium occupation on octahedral sites in the spinel phase is negligibly small.

The atomic fractions deduced from refined site occupations show that (i) this sample is stoichiometric $LiMn_2O_4$ within experimental error ($\alpha = 0$); (ii) it contains ca. 3% (by weight) Li_2MnO_3. The decrease in lithium content (from

TABLE 2
Results of Rietveld Refinements from Neutron Diffraction Data on $Li_{1.05}Mn_2O_{4-\delta}$ Samples

Space group cell parameters (Å)	Atom	Site	x	y	z	Site occupancy	B_{iso} (Å^2)	Formula
				Sample T800SC				
$Fd\bar{3}m$	Li(1)	8*a*	0.125	0.125	0.125	1	0.96(11)	LiM_2O_4
$a = 8.2232(4)$	Li(2)	16*c*	0.5	0.5	0.5	0.06(3)	0.27(3)	$M_2 = Mn_{1.88(6)}Li_{0.12(6)}$
$z = 8$	Mn	16*c*	0.5	0.5	0.5	0.94(3)	0.27(3)	
	O	32*e*	0.2633(4)	0.2633(4)	0.2633(4)	1.00(7)	0.92(1)	
$N - P + C = 2935$, $R_p = 4.58$, $R_{wp} = 5.92$, $R_{exp} = 1.93$, $R_{Bragg} = 4.80$; 41 spinel reflections used in the refinement.								
				Sample T800Q				
$Fd\bar{3}m$	Li	8*a*	0.125	0.125	0.125	1.00(1)	1.08(10)	$LiMn_2O_4$ (97.1 wt%)
$a = 8.2449(2)$	Mn	16*c*	0.5	0.5	0.5	0.99(1)	0.36(3)	$+ Li_2MnO_3$ (2.9 wt%)
$z = 8$	O	32*e*	0.2632(3)	0.2632(3)	0.2632(3)	1	1.22(1)	
$N - P + C = 2774$, $R_p = 3.75$, $R_{wp} = 4.93$, $R_{exp} = 1.46$, $R_{Bragg} = 3.44$; 41 spinel reflections used in the refinement.								
				Sample T925Q				
$I4_1/amd$	Li	4*a*	0	0.750	0.125	0.89(3)	0.80(10)	$Li_{0.89(3)}Mn_2O_{3.84(8)}$ (91 wt%)
$a = 5.7396(2)$	Mn	8*d*	0	0	0.5	1	0.80(10)	$+ Li_2MnO_3$ (9 wt%)
$c = 8.6709(6)$	O	16*h*	0	0.4734(3)	0.2608(3)	0.96(2)	[a]	
$z = 4$								
$N - P + C = 2794$, $R_p = 6.29$, $R_{wp} = 8.48$, $R_{exp} = 1.89$, $R_{Bragg} = 11.1$; 88 spinel reflections used in the refinement.								

[a] Oxygen anisotropic displacement coefficients ($\times 10^4$): $\beta_{11} = 40(3)$, $\beta_{22} = 34(3)$, $\beta_{33} = 103(2)$, $\beta_{12} = 0$, $\beta_{13} = 0$, $\beta_{23} = 27(6)$.

$\alpha = 0.12$ to $\alpha = 0$) and the simultaneous emergence of Li_2MnO_3 correspond to the reaction

$$Li_{1+\alpha}Mn_{2-\alpha}O_4 \rightarrow (1-\alpha)\,LiMn_2O_4 + \alpha\,LiMnO_3 + (\alpha/2)\,O_2.$$

The proportions of $LiMn_2O_4$ and Li_2MnO_3 deduced from this reaction with $\alpha = 0.12$ are consistent with the fractions obtained from the Rietveld refinement. This result shows that, in this temperature range, the mass loss is *not due to the formation of oxygen vacancies*, but corresponds to a change in spinel stoichiometry toward Li-poorer compositions, while the overall stoichiometric ratio cation/anion = 3/4 is maintained. The shift to lower α and the simultaneous decrease in manganese oxidation state v(Mn) in the spinel phase are compensated by the formation of a second, lithium-richer phase Li_2MnO_3 and by liberation of oxygen, in agreement with thermogravimetric observations (6).

Sample T925Q. Comparing Figs. 1b and 1c, one immediately notes a splitting of most spinel reflections in the latter. Its powder pattern is indexable in a hausmannite-type cell (space group $I4_1/amd$).

The structure was first refined with full manganese octahedral site occupation and an overall isotropic displacement parameter. Refining these variables led to much higher R-factors than in previous cases ($R_{wp} = 17.0$, instead of 4.93 for T800Q, see Table 2). Various attempts showed that this poor agreement was not due to cation distribution, orientation effects or a wrong space group choice.

Difference Fourier maps, however, clearly show the presence of residual elongated nuclear densities near the oxygen atom site along the z direction (see Fig. 2). Introducing oxygen anisotropic displacement parameters in the structural model led to a considerable drop in reliability factors ($R_{wp} = 8.48$). The corresponding difference pattern is given in Fig. 1c. The final β_{ij} coefficient values (see Table 2) correspond to an atomic displacement ellipsoid around the oxygen position with main axes almost parallel with the unit cell directions. The strong anisotropy in B (0.52, 0.34, and 3.19 Å^2 along x, y, and z, respectively) is probably due to a static disorder of the oxygen atoms, which could be induced by the presence of vacancies.

In all cases indeed, the refinement leads to a cation/anion ratio slightly larger than 3/4, corresponding to oxygen vacancies. The average manganese oxidation state is 3.35, consistent with a Jahn–Teller distorted tetragonal structure (1). The reaction between 800 and 925°C can be written

$$(3+x)LiMn_2O_4 \rightarrow 3Li_{1-x}Mn_2O_{4-y} + 2xLi_2MnO_3 + \delta O_2$$

with $\delta = 1.5y - x$. Such a reaction is in agreement with an increase in the Li_2MnO_3 content in the sample.

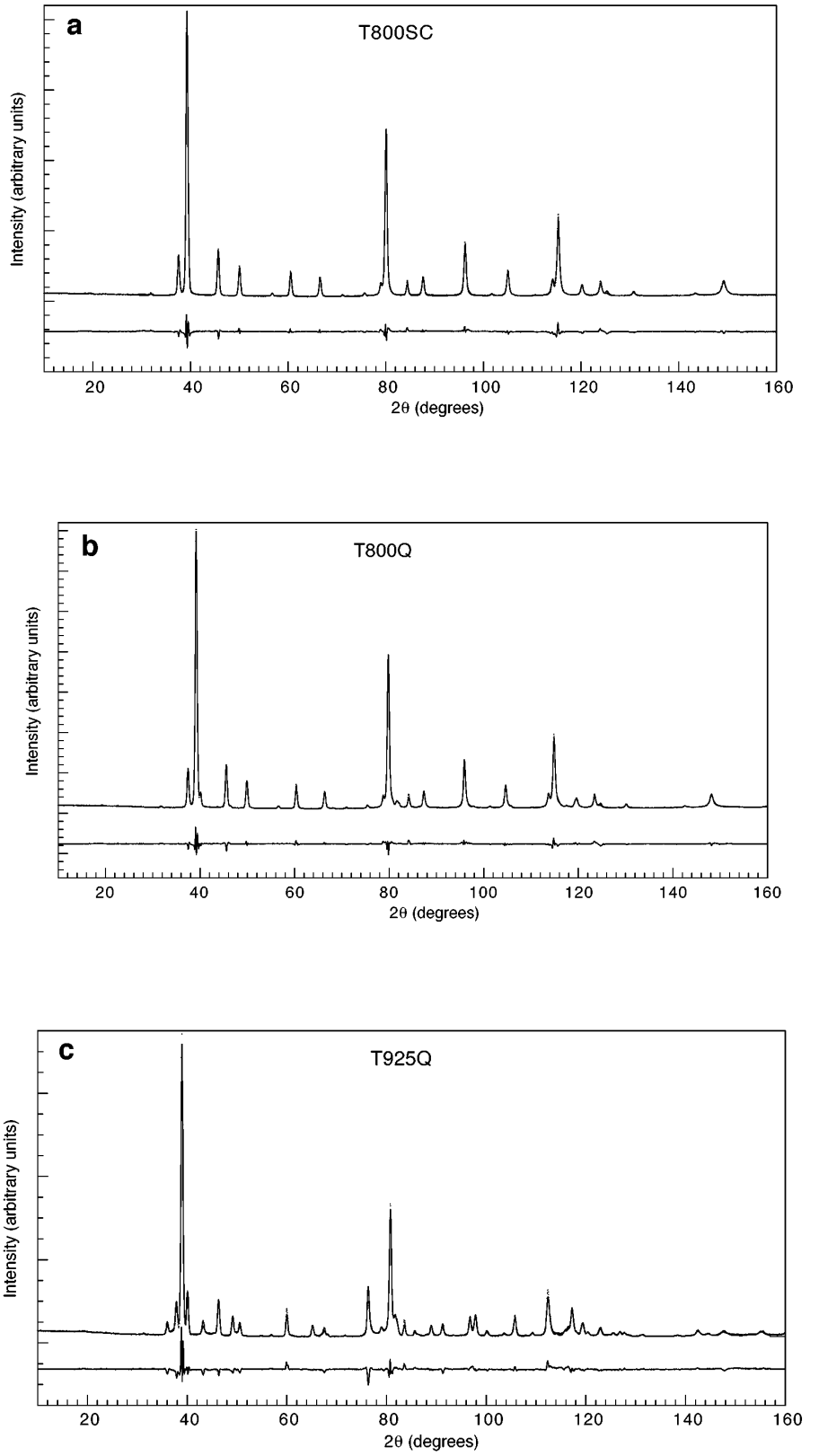

FIG. 1. Observed (points) and calculated (continuous line) neutron powder patterns of samples T800SC (top), T800Q (middle), and T925Q (bottom). The lower field shows the difference $I_{obs} - I_{calc}$.

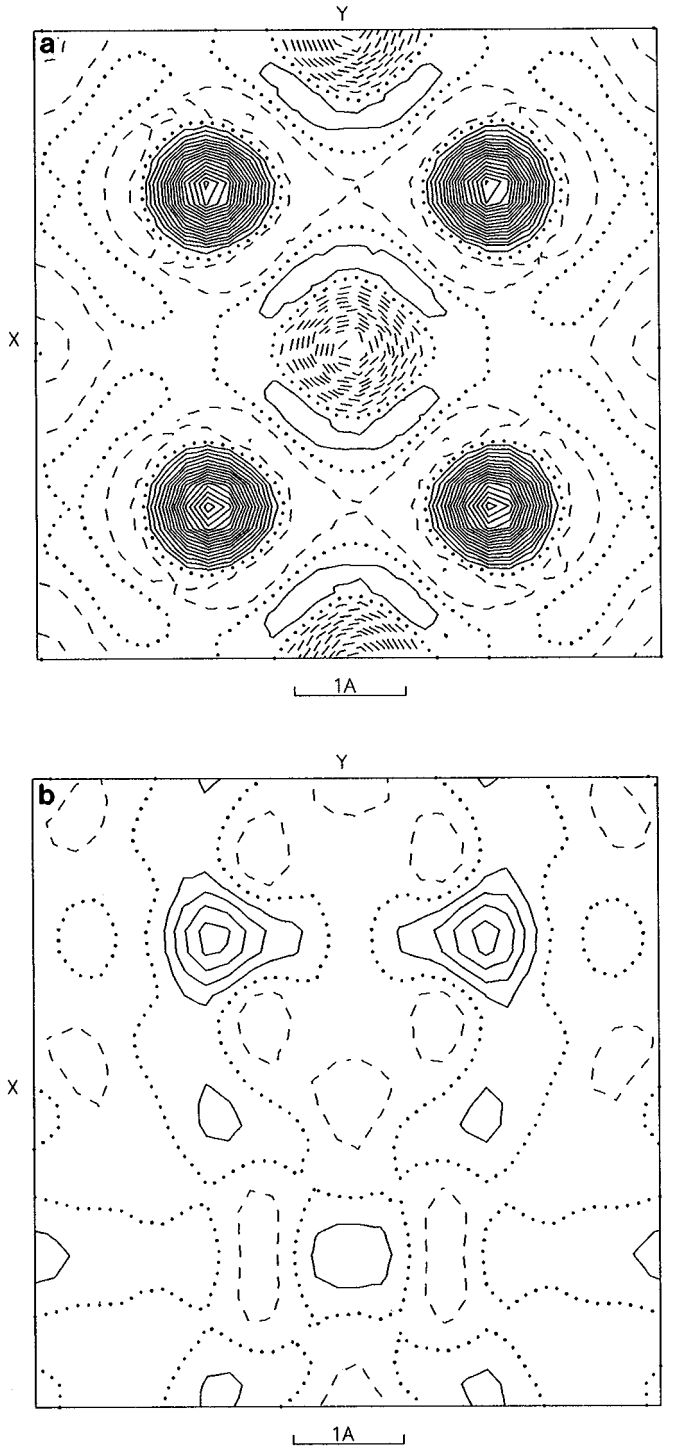

FIG. 2. Fourier maps determined from the neutron powder pattern of sample T925Q. (a) Fourier section for $z = 0$; (b) difference map at $z = 0.05$, showing residual nuclear density around the oxygen atom positions along the z axis.

2. *Ammonia-Treated Spinel*

As mentioned in the experimental section, sample C also contains Li_2MnO_3 as a second phase. This impurity is difficult to detect in the diffraction patterns, because the monoclinic Li_2MnO_3 structure derives from a rocksalt-type subcell with a cell parameter close to *a*(spinel)/2 (13), resulting in considerable overlap of reflections with the spinel ones. The structures of both samples C and CN (ammonia-treated) were refined satisfactorily with the cubic spinel model. Residuals were significantly lowered with Li_2MnO_3 included in the refinement. The mass fraction of the latter in sample C was found to lie in the 10–15% range. The results of refinements on samples C and CN are summarized in Table 3, and difference powder patterns are shown in Fig. 3.

Regarding sample C, the tetrahedral sites were assumed fully occupied. Refining independently the Li2 and Mn occupations in the spinel phase did not result in significant shifts from (Li2 + Mn) = 1. These occupations were therefore constrained to full occupation of the 16d sites in the subsequent refinements. These showed that the spinel phase in sample C is stoichiometric in oxygen, within experimental errors (experimental value: 3.97(7) oxygen atoms per spinel formula unit). As expected, its cation distribution is characterized by a value of α (0.20) significantly lower than the nominal value 1/3, and corresponds to a manganese average oxidation state equal to 3.75. The stoichiometry of the spinel phase and the Li_2MnO_3 mass fraction are consistent with the overall composition, i.e.,

$$6Li_{1.33}Mn_{1.67}O_x = 5Li_{1.2}Mn_{1.8}O_4 + Li_2MnO_3.$$

The oxygen position parameter is slightly lower than those observed in the high-temperature samples T800SC and T800Q; this difference can be ascribed to the higher lithium content on octahedral sites in the case of sample C. The cell parameter of $Li_{1.2}Mn_{1.8}O_4$ (8.149 Å) is also significantly lower than that obtained for Li–Mn–O samples with similar stoichiometry prepared at high temperature (6, 14). In the latter case, a large fraction of Li_2MnO_3 is formed and the actual α value in the spinel phase is lower than 0.20. The influence of synthesis temperature on the Li/Mn ratio in Li–Mn–O spinels has been discussed recently by Endres *et al.* (14) and by Le Cras *et al.* (15).

The neutron powder pattern of the ammonia-treated sample CN was refined using the same strategy. The results (see Table 3) show a number of significant changes with respect to sample C: (i) an increase in cell parameter, (ii) a significant decrease in oxygen occupancy, (iii) an increase in α value (from 0.20 to 0.28), (iv) an increase in the atomic displacement parameters of oxygen and tetrahedral lithium atoms. This refinement confirms the work of Richard *et al.*, who concluded from X-ray data that oxygen vacancies occur in the spinel structure (9). The refined atomic occupations yield a decrease in average manganese valence in the spinel phase from 3.75 to 3.63 as a result of the ammonia treatment. Taking into account the Li_2MnO_3 fraction, the expected oxygen loss is then 4.1%, in fairly good agreement

TABLE 3
Results of Rietveld Refinements of Neutron Diffraction Data on $Li_{0.28}Mn_{1.72}O_{4-\delta}$ Samples

Space group cell parameters (Å)	Atom	Site	x	y	z	Site occupancy	B_{iso} (Å^2)	Formula
				Sample C				
$Fd\bar{3}m$	Li1	8*a*	0.125	0.125	0.125	1	0.52(11)	LiM_2O_4
$a = 8.1491(4)$	Li2	16*c*	0.5	0.5	0.5	0.099(36)	0.65(4)	$M_2 = Mn_{1.80(7)}Li_{0.20(7)}$ (88 wt%)
	Mn	16*c*	0.5	0.5	0.5	0.901(36)	0.65(4)	+ Li_2MnO_3 (12 wt%)
	O	32*e*	0.26251(4)	0.26251(4)	0.26251(4)	0.993(18)	1.26(2)	
$N - P + C = 2889$, $R_p = 4.20$, $R_{wp} = 4.14$, $R_{exp} = 1.33$, $R_{Bragg} = 4.33$; 39 spinel reflections used in the refinement.								
				Sample CN				
$Fd\bar{3}m$	Li1	8*a*	0.125	0.125	0.125	1	1.26(15)	$LiM_2O_{3.74(7)}$
$a = 8.1634(5)$	Li2	16*c*	0.5	0.5	0.5	0.144(36)	0.61(5)	$M_2 = Mn_{1.72(7)}Li_{0.28(7)}$ (86 wt%)
	Mn	16*c*	0.5	0.5	0.5	0.858(36)	0.61(5)	+ Li_2MnO_3 (14 wt%)
	O	32*e*	0.26196(6)	0.26196(6)	0.26196(6)	0.933(18)	1.61(2)	
$N - P + C = 2932$, $R_p = 3.65$, $R_{wp} = 4.61$, $R_{exp} = 1.28$, $R_{Bragg} = 3.86$; 39 spinel reflections used in the refinement.								

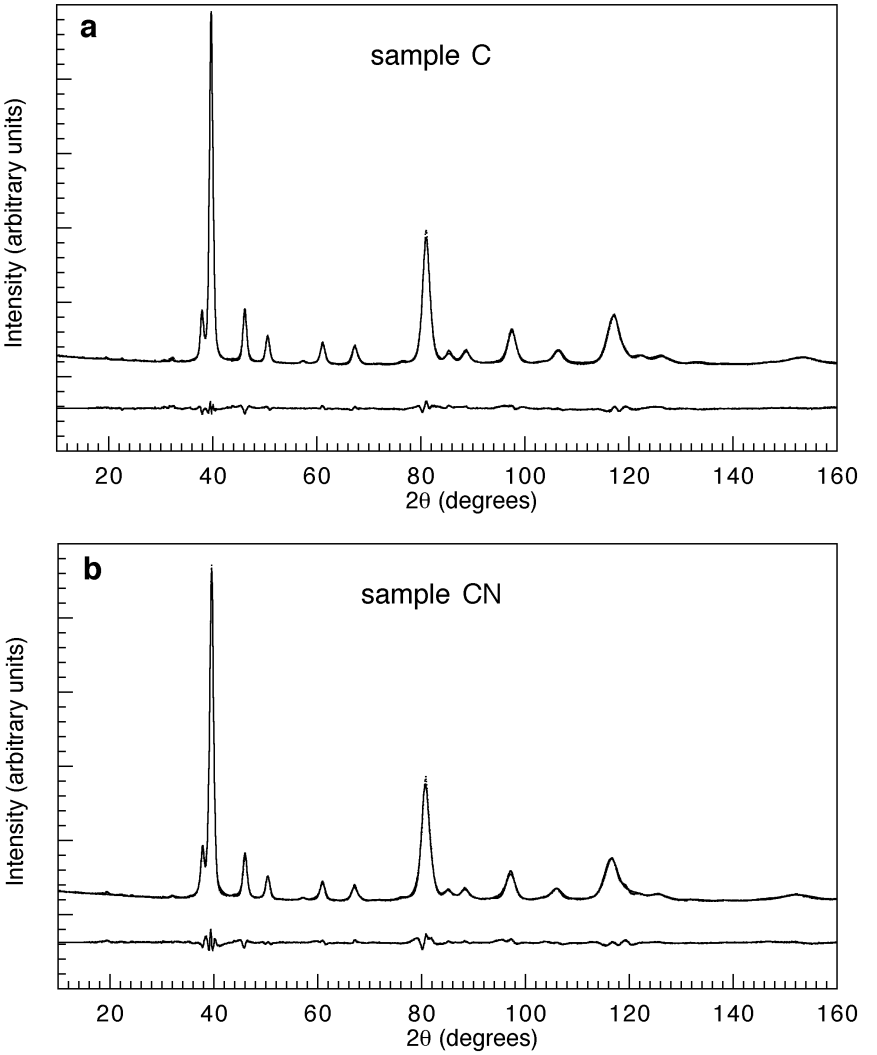

FIG. 3. Observed (points) and calculated (continuous line) neutron powder patterns of samples C (top) and CN (bottom). The lower field shows the difference $I_{obs} - I_{calc}$.

with the 3.0% weight loss measured directly. The increase in cell parameter can be ascribed to this manganese oxidation state change, since a decrease in charge on the manganese atoms results in a lengthening of the Mn–O interatomic distances.

The presence of 0.067 vacancies on the oxygen sites can also explain the increased atomic displacement parameter observed on this sites, as already noted in oxygen-deficient T925Q. In the latter, this atomic displacement is markedly anisotropic. No evidence of such anisotropy is observed for sample CN. This discrepancy is probably related to another important difference between samples CN and T925Q: cubic symmetry is maintained in the former, while it is lowered to tetragonal in the latter.

DISCUSSION

It is interesting to compare the two processes of thermal deoxygenation and ammonia reduction in a composition–valence diagram (16). This diagram (see Fig. 4) clearly shows the important difference between the reaction mechanisms T800SC → T800Q and T800Q → T925Q. The former reaction corresponds to a cation distribution rearrangement (change in Li/Mn ratio) while maintaining the spinel composition on the stoichiometric M_3O_4 line. In the latter reaction, in contrast, the composition leaves this line to enter the anion-defective domain. In the C → CN reaction, these two effects are combined since the oxygen extraction is accompanied by a Li/Mn increase in the spinel phase.

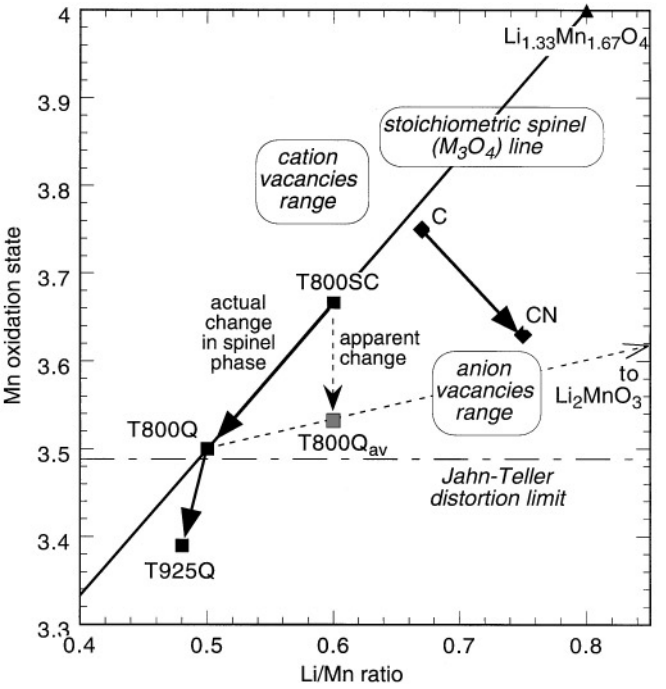

FIG. 4. Composition–valence diagram for the Li–Mn–O system. Bold line: $Li_{1+\alpha}Mn_{2-\alpha}O_4$ stoichiometry. The bold arrows show the composition change on quenching or ammonia treatment (squares: T800/925 series; diamonds: C series). $T800Q_{av}$ = average global composition of the two-phase sample T800Q.

The compensating effect of Li_2MnO_3 is easily demonstrated on the composition–valence diagram. As indicated for the T800SC–T800Q reaction in Fig. 4, the overall, apparent composition moves down into the anion-deficient region (dashed line to point $T800Q_{av}$) as a result of oxygen loss. This point, however, does not represent an actual phase composition, but rather the center of gravity of the two-phase mixture T800Q (which actually lies on the stoichiometric spinel line) + Li_2MnO_3. Finally, this diagram also displays the Jahn-Teller distortion limit (just below the 3.5 manganese valence line), which is crossed here in sample T925Q, but not in sample CN.

CONCLUSION

We showed in this study that lithium manganese spinel oxides can indeed lose oxygen, either by annealing and quenching at high temperature, or by low-temperature treatment with a reducing gas such as ammonia. The solid–gas equilibrium, however, is more complex than a simple oxygen extraction from a host with constant cation composition: the oxygen content variation is always accompanied by simultaneous changes in (i) Li/Mn ratio in the spinel phase and (ii) the proportion of Li_2MnO_3 present in the system. The flexibility of the spinel structure, with variable *B*-site cation distribution, makes the mechanism of oxygen exchange in this system quite different from that in perovskite-related cuprates such as the $YBa_2Cu_3O_{7-x}$ system, where the oxygen content can be varied in a wide range without change in cation occupations (17–19).

ACKNOWLEDGMENTS

The authors thank Peter Cross and Jean Pannetier for their assistance in the neutron diffraction experiments at Institut Laue-Langevin, Grenoble.

REFERENCES

1. M. M. Thackeray, *Prog. Batteries Battery Mater.* **11,** 150 (1992).
2. D. Guyomard and J. M. Tarascon, *Solid State Ionics* **69,** 222 (1994).
3. J. C. Hunter, *J. Solid State Chem.* **39,** 142 (1981).
4. A. De Kock, M. Rossouw, L. A. de Picciotto, M. M. Thackeray, W. I. F. David, and R. M. Ibberson, *Mater. Res. Bull.* **25,** 657 (1990).
5. F. Le Cras, D. Bloch, M. Anne, and P. Strobel, *Mater. Soc. Symp. Proc.* **369**, 39 (1995).
6. J. M. Tarascon, W. R. Mckinnon, F. Coowar, T. N. Bowmer, G. Amatucci, and D. Guyomard, *J. Electrochem. Soc.* **141,** 1421 (1994).
7. J. Sugiyama, T. Atsumi, T. Hioki, S. Noda, and N. Kamegashira, *J. Alloys Comp.* **235,** 163 (1996).
8. M. M. Thackeray, M. F. Mansuetto, D. W. Dees, and D. R. Vissers, *Mater. Res. Bull.* **31,** 133 (1996).

9. M. Richard, E. W. Fuller, and J. R. Dahn, *Solid State Ionics* **73,** 81 (1994).
10. T. Takada, H. Hayakawa, T. Kumagai, and E. Akiba, *J. Solid State Chem.* **121,** 79 (1995)
11. F. Le Cras, P. Strobel, M. Anne, D. Bloch, J. B. Soupart, and J. C. Rousche, *Eur. J. Solid State Inorg. Chem.* **33,** 67 (1996).
12. J. Rodriguez-Carvajal, "Satellite Meeting of the 15th Congress of the IUCr, Toulouse, France," p. 127, 1990.
13. P. Strobel and B. Lambert-Andron, *J. Solid State Chem.* **77,** 33 (1988).
14. P. Endres, B. Fuchs, S. Kemmler-Sack, G. Faust-Becker, and H. W. Praas, *Solid State Ionics* **89,** 221 (1996).
15. F. Le Cras, D. Bloch, and P. Strobel, *J. Power Sources* **63,** 71 (1996)
16. P. Strobel, F. Le Cras, and M. Anne, *J. Solid State Chem.* **124,** 83 (1996).
17. P. Strobel, J. J. Capponi, C. Chaillout, M. Marezio, and J. L. Tholence, *Nature* **327,** 306 (1987).
18. A. Manthiram, J. S. Swinnea, Z. T. Sui, H. Steinfink, and J. B. Goodenough, *J. Am. Chem. Soc.* **109,** 6667 (1987).
19. R. J. Cava, A. W. Hewat, E. A. Hewat, B. Batlogg, M. Marezio, K. M. Rabe, J. J. Krajewski, W. F. Peck, and L. W. Rupp, *Physica C* **165,** 419 (1990).